DETERMINATION OF TWIN TURBOPROP UTILITY AIRCRAFT WHIRL FLUTTER STABILITY BOUNDARIES

Jiri Cecrdle, Ph.D.*
***Aeronautical Research and Test Institute (VZLU), Prague, Czech Republic;**
tel.: (+420) 225 115 123; e-mail: cecrdle@vzlu.cz

Keywords: *aeroelasticity, flutter, whirl flutter, EV-55 aircraft*

Abstract

The submitted paper deals with the aircraft structure whirl flutter analysis. It gives a summary of the regulations requirements, the theoretical background and the aircraft certification relating issues. The main part deals with the whirl flutter analyses of the new twin turboprop utility aircraft. The optimization based analytical procedure to determine the whirl flutter stability boundaries for the certification speed is employed. Finally, the propeller – nacelle - wing interference effects (downwash) are evaluated and the future work is outlined.

1 Introduction

The turboprop aircraft are required to be certified considering the whirl flutter. Rotating parts like a propeller or a turbine increase the number of degrees of freedom and cause additional forces and moments. Moreover rotating propeller causes a complicated flow field and interference effects between wing, nacelle and propeller. Whirl flutter may cause the propeller mounting unstable vibrations, even a failure of the engine, nacelle or whole wing. It has been the cause of a number of accidents (two Lockheed Electra II airliners in 1959 and 1960 and a Beech 1900C commuter in 1991).

Airworthiness regulations require taking into account the influence of the rotational degrees of freedom of the propeller plane and significant elastic, inertia and aerodynamic forces. Also the changes in the stiffness and damping of the propeller – engine – nacelle – structure system must be considered (§23.629(e)(1)(2)).

However, at the utility aircraft category, the reliable stiffness data regarding the engine attachment (engine mount-isolators, engine bed etc.) are not at disposal until the ground vibration test of the prototype, when the final updating of the analytical model is possible. Nevertheless, considering the timesaving in the final development phase, it is worth to perform the whirl flutter calculations in the earlier phase. For this purpose, the optimization-based analytical procedure for determination of the critical values of engine attachment stiffness parameters (or the engine vertical and lateral vibration frequencies) has been prepared [9]. It allows determination of the whirl flutter and divergence stability boundaries for the speed, which is set by regulations as a certification speed. Later on, calculated critical values can be compared with the prototype experimental results, especially from the ground vibrations tests. Mentioned procedure has been employed during development and certification of the new Czech twin utility turboprop aircraft.

2 Theoretical Background

Engine flexible mounting is represented by two rotational springs (stiffness K_Ψ, K_Θ) as illustrated in the fig.1. Propeller is considered as rigid; rotating with angular velocity Ω. System is exposed to the airflow of velocity V_∞ [3], [4].

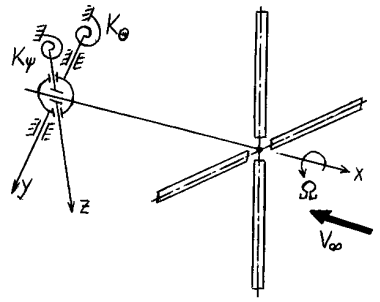

Fig.1. Gyroscopic system with propeller

Neglecting propeller rotation and the aerodynamic forces, the two independent mode shapes (yaw – around vertical axis, pitch – around lateral axis) will emerge with angular frequencies ω_Ψ and ω_Θ. Considering the propeller rotation, the primary system motion changes to the characteristic gyroscopic motion. The gyroscopic effect makes two independent mode shapes merge to whirl motion. The propeller axis shows an elliptical movement. The orientation of the propeller axis movement is backward relatively to the propeller rotation for the mode with lower frequency (backward whirl mode) and forward relatively to the propeller rotation for the mode with higher frequency (forward whirl mode). The mode shapes of gyroscopic modes are complex, since independent yaw and pitch modes have a phase shift 90°. Condition of real mode shapes corresponds to the state of the non-rotating system.

The described gyroscopic mode shapes make harmonic changes of propeller blades angles of attack. They give rise to non-stationary aerodynamic forces, which may under the specific conditions induce a whirl flutter. Possible states of the gyroscopic system from the flutter stability point of view for backward mode are explained in the fig.2.

Provided that the air velocity is lower than

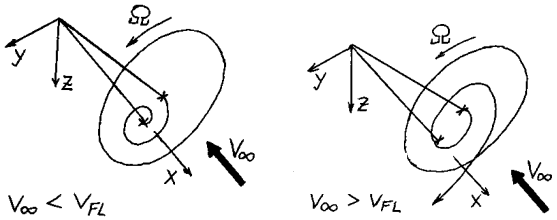

Fig.2. Stable and unstable state of gyroscopic vibrations for backward flutter mode

critical value ($V_\infty < V_{FL}$), the system is stable and the motion is damped. If the airspeed exceeds the critical value ($V_\infty > V_{FL}$), the system becomes unstable and motion is diverging. The limit state ($V_\infty = V_{FL}$) with no total damping is called critical flutter state and V_{FL} is called critical flutter speed.

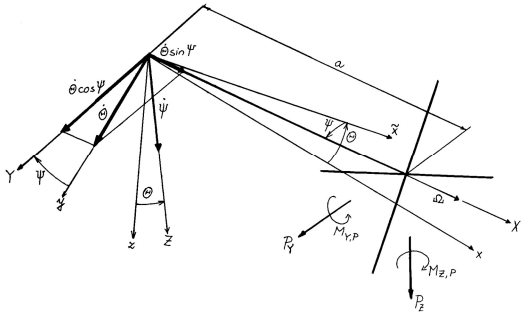

Fig.3. Kinematical scheme of the gyroscopic system

The basic problem of the analytical solution consists in the determination of the aerodynamic forces caused by the gyroscopic motion for propeller blades. The equations of motion were set up for system described in the fig.1. The kinematical scheme including gyroscopic effects is shown in the fig.3. The independent generalized coordinates are three angles (φ, Θ, Ψ). We assume the propeller angular velocity constant (φ = Ωt), mass distribution symmetric around X-axis and mass moments of inertia $J_Z \neq J_Y$.

Considering the small angles simplification, the equations of motion become:

$$\begin{aligned} J_Y\ddot{\Theta}+\frac{K_\Theta\gamma_\Theta}{\omega}\dot{\Theta}+J_X\Omega\dot{\Psi}+K_\Theta\Theta &= M_{Y,P}-a.P_Z \\ J_Z\ddot{\Psi}+\frac{K_\Psi\gamma_\Psi}{\omega}\dot{\Psi}-J_X\Omega\dot{\Theta}+K_\Psi\Psi &= M_{Z,P}+a.P_y \end{aligned} \qquad (1)$$

We formulate the propeller aerodynamic forces by means of the aerodynamic derivatives [1], [2] and make the simplification for the harmonic motion, and then the final whirl flutter matrix equation will become:

$$\left(-\omega^2[M]+j\omega\left([D]+[G]+q_\infty F_P\frac{D_P^2}{V_\infty}[D^A]\right)+ +\left([K]+q_\infty F_P D_P[K^A]\right)\right)\times\begin{bmatrix}\Theta\\ \Psi\end{bmatrix}=\{0\} \qquad (2)$$

The limit state emerges for the specific combination of parameters V_∞ and Ω, when the angular velocity ω is real. The whirl flutter characteristics are explained in the fig.4, which describes influence of the propeller advance ratio (V_∞ / (ΩR)) on the stability of undamped gyroscopic system. Increasing the propeller advance ratio requires an increase of the necessary stiffnesses K_Θ, K_Ψ. Also influences of the structural damping and a distance propeller – mode shape node are significant.

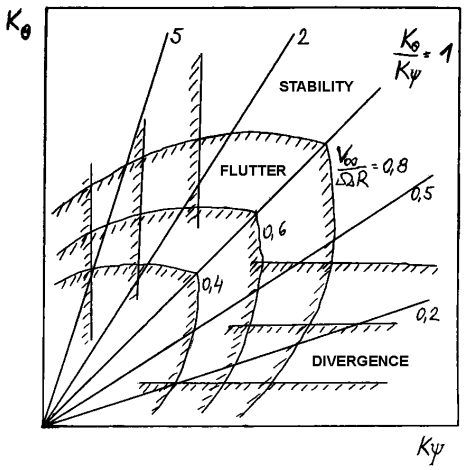

Fig.4. Influence of the propeller advance ratio (V_∞/(ΩR)) to the stability of undamped gyroscopic

The whirl flutter appears at the gyroscopic rotational vibrations, the flutter frequency is the same as the frequency of the backward gyroscopic mode. The critical state may be reached either due to increasing the air velocity or the propeller revolutions. Structural damping is a significant stabilization factor. On the contrary, the propeller thrust influence is barely noticeable. The most critical state is $K_\Theta = K_\Psi$, it means $\omega_\Theta = \omega_\Psi$ when the interaction of both independent motions is maximal. A special case of the eq.(2) for ω=0 is the gyroscopic static divergence.

3 Analytical Procedure

Analytical approach is based on the NASTRAN program system. The standard whirl flutter solution employing the NASTRAN flutter solver (SOL 145) grounds on the Strip Aerodynamic Theory for the propeller at the windmilling mode. A propeller is assumed rigid. For the residual structure a Wing – Body Interference Aerodynamic Theory is used. For the flutter stability solution the PK method is applied. The NASTRAN whirl flutter DMAP (Direct Matrix Abstraction Program) subroutine is supplemented by the external preprocessor (program propfm) for calculation of the propeller aerodynamic matrices (formally damping and stiffness matrices) and optionally for calculation of the down / side wash effects.

The FE model is prepared similarly as for the standard flutter analysis; the model must include the node at the propeller center of gravity with propeller mass characteristics. Data for calculation of downwash and sidewash angles may be specified by means of the partitioning matrices. The first NASTRAN run calculates the down / side wash angles only. These data and other data concerning the engine and the propeller are inputs to the external preprocessor. Output data from preprocesor are added to the NASTRAN input, formally as a direct input to the stiffness and damping matrices. Partitioning matrices must be removed. The second NASTRAN run is the final one and consist in the flutter stability calculation.

The propeller aerodynamic forces and moments are calculated by eq.(3):

$$
\begin{aligned}
P_Y &= q_\infty F_p \left(c_{y\Psi}\Psi^* + c_{y\Theta}\Theta^* + c_{yq}\frac{\dot{\Theta}^* R}{V_\infty} \right) \\
P_Z &= q_\infty F_p \left(c_{z\Theta}\Theta^* + c_{z\Psi}\Psi^* + c_{zr}\frac{\dot{\Psi}^* R}{V_\infty} \right) \\
M_{Y,P} &= q_\infty F_P D_P \left(c_{m\Psi}\Psi^* + c_{mq}\frac{\dot{\Theta}^* R}{V_\infty} \right) \\
M_{Z,P} &= q_\infty F_P D_P \left(c_{n\Theta}\Theta^* + c_{nr}\frac{\dot{\Psi}^* R}{V_\infty} \right)
\end{aligned}
\qquad (3)
$$

Aerodynamic derivatives are given from propeller blade integrals [5], effective angles are shown in the fig.5.

An option to include the downwash and sidewash effects may be important for configuration with engines mounted to the wing.

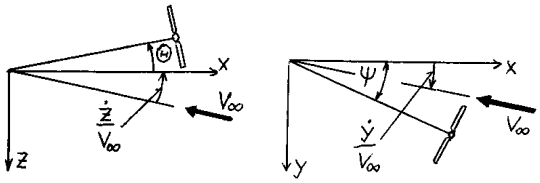

Fig.5. Effective static angles

Downwash and sidewash angles behind the propeller describe interference between propeller and nacelle. Induced downwash and sidewash angles are added to the effective static angles (fig.5) by the eq.(4):

$$\Theta^* = \Theta + \frac{\dot{z}}{V_\infty} - \frac{w_1}{V_\infty}$$
$$\Psi^* = \Psi - \frac{\dot{y}}{V_\infty} + \frac{w_2}{V_\infty} \qquad (4)$$

Above mentioned induced down / side wash angles dependent on the reduced frequency can be obtained from the lift solution by partitioning the interference coefficients. The downwash effect influences only the aerodynamic stiffness matrix; influence to the aerodynamic damping matrix is neglected.

Application of the NASTRAN optimization solver (SOL 200) to the whirl flutter solution makes possible calculation of the flutter stability boundaries for the specified certification speed as described in the fig.6. Such approach allows to easily evaluating the influence of the secondary parameters to the whirl flutter stability.

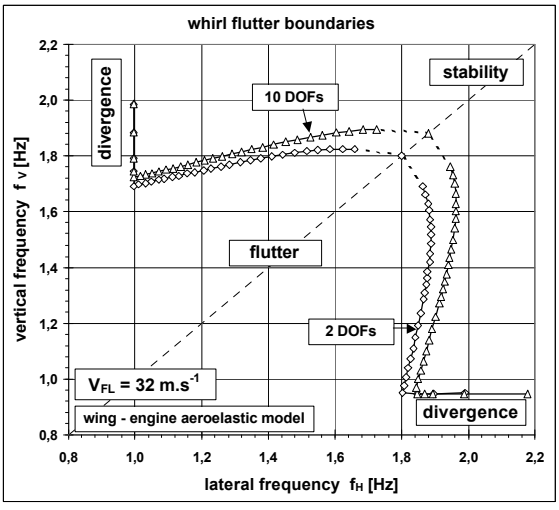

Fig.6. Whirl flutter / divergence boundary – optimization solution – approach description

The basic flutter equation of the PK method in modal coordinates is:

$$\left[M_{hh} p^2 + \left(B_{hh} - \frac{1}{4} \frac{\rho c V Q_{hh}^{Im}}{k} \right) p + \right.$$
$$\left. + \left(K_{hh} - \frac{1}{2} \rho V Q_{hh}^{Re} \right) \right] \{u_h\} = 0 \qquad (5)$$

M_{hh}, B_{hh} and K_{hh} are modal mass, damping and stiffness matrices respectively. Aerodynamic loads are incorporated into damping and stiffness matrices. Aerodynamic matrices are dependent on the reduced frequency (k) at a gentle rate. All matrices are real; Q_{hh}^{Re} and Q_{hh}^{Im} are real and imaginary part of a complex aerodynamic matrix Q_{hh}. The decay rate coefficient is defined in connection with the complex eigenvalue:

$$p = \omega(\gamma \pm j) = p^{Re} + j\, p^{Im} \qquad (6)$$

Flutter sensitivities are computed as rate of change of the transient decay coefficient γ with respect to changes in design variables ($\partial\gamma/\partial x_i$).

The most important parameters influencing the whirl flutter are the natural frequencies of the engine vertical and lateral vibration modes; and also a ratio of both ones. Let's assume the inertia characteristics of the engine – propeller system and the residual structure reliably determined. That's why the engine suspension stiffness parameters would be used as optimization parameters. We formulate two design variables: the rotational stiffness of the engine attachment around the vertical and lateral axes ($K_{\varphi V}$, $K_{\varphi H}$). Design properties and the relations to the design variables are to be defined in accordance with the stiffness model type (two springs, system of springs, beams, shells, combined model, etc.).

Firstly, the target frequency ratio (TFR) is tuned by means of the NASTRAN optimization for normal modes. Design variable is either $K_{\varphi V}$ or $K_{\varphi H}$. The objective function is defined as:

$$min(ABS((FREQ2/FREQ1) - TFR)) \qquad (7)$$

where FREQx are both engine vibration frequencies (vertical - f_V and lateral - f_H), FREQ2 is higher one, FREQ1 is lower one. It is obvious, that the TFR > 1, so the order of both frequencies must be taken under consideration.

The output from this phase is the initial value of $K_{\varphi V}$ and $K_{\varphi H}$ for the main optimization. The ratio of both frequencies (f_V and f_H) is equal to the TFR. The main optimization step follows the preparatory one. It is the NASTRAN optimization (SOL 200) composite solution of both normal modes and aeroelastic flutter solution. The modal subcase includes the design constraint to keep the frequency ratio defined as:

$$(0.98*TFR<(FREQ2/FREQ1)<1.02*TFR) \quad (8)$$

and also the objective function defined as:

$$min(FREQ1+FREQ2) \quad (9)$$

The flutter subcase includes constraint to keep the flutter stability for all included modes at the certification velocity ($1.2*V_D$), it means $g < 0$, defined as:

$$(-\infty<((g(1.2*V_D)-0.03)/0.1)<-0.3)) \quad (10)$$

The interval shift from the null value is applied due to the numeric character of the solution. This constraint prevents also from the other type of flutter instability below the certification speed, which may be caused by the design variables changes. Whirl flutter calculation is performed only for one velocity ($1.2*V_D$). Obviously, the solution must include all the data as the ordinary whirl flutter solution (DMIG cards from propfm etc.). For the NASTRAN SOL 200, the DMAP alter was adapted (propa_200.alt). The outputs from this phase are final stiffness parameters ($K_{\varphi V}$ and $K_{\varphi H}$) and corresponding frequencies f_V and f_H. Frequency ratio is equal to the TFR. At the same time, the critical flutter speed is equal to the certification speed ($V_{FL} = 1.2*V_D$). It is applicable for the divergence as well. After optimization, it is recommended to perform a standard whirl flutter solution for standard number of velocities to check the flutter behavior of the updated structure. Described procedure is required to be repeated for the range of target frequency ratios, the order of the vertical and lateral modes (lower, higher) must be taken in account as well. The described procedure is applicable for no downwash option.

Provided the downwash effect is included, the procedure is enlarged by additional steps. It is assumed, that the influence of the downwash is not a crucial point and have only partial influence. That's why the downwash data are calculated just for the state optimized for no downwash option. These data are remained for the rest of the procedure. Firstly, the downwash data are calculated by means of the standard flutter solver. Then downwash data are included to the propfm program input data and the propeller aerodynamic matrices including the downwash effect are calculated. Then the main optimization step is repeated, the initial design variables are those ones tuned for the no downwash option. The final values represent the optimized structure including the downwash. Finally, standard whirl flutter solution for to check the flutter behavior of the updated

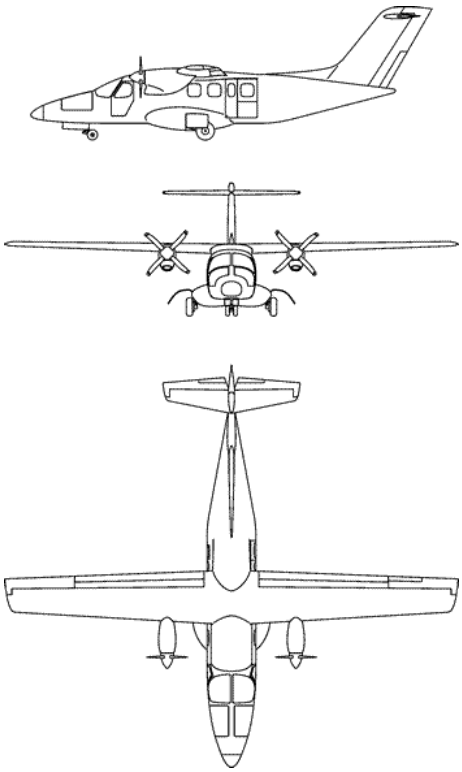

Fig.7. EV-55 aircraft outline

structure is recommended.

The downwash angles are to be calculated for each target ratio separately, so it is obvious, that the downwash including option makes the calculation much larger. On the other side, as described later, the influence of the downwash is in most cases destabilizing. Considering this, it is recommended to make a downwash including calculation at least for the selected (critical) configurations of the residual structure.

4 Application to the EV-55 Aircraft Structure

The EV-55 „Outback“ (see fig.7) is a new generation Czech twin turboprop aircraft designed and manufactured by the Evektor Kunovice, supported by other companies joined in the Association of Aviation Manufacturers of the Czech republic. EV-55 is designed as more reliable and powerful than existing same-class machines. This low-priced and low operation costs small civil transport aircraft is intended for small operators, especially those providing services on demand. Different kind of operation like passenger, cargo or combi can be equally envisaged. With a total length of 14.35 m, and the wingspan of 16.10 m and MTOW 4600 kg, EV-55 will travel with maximum speed of over 220 kts. The power unit consists of the turboprop engines P&WC PT6A-21 (536 shp each) and the four-blade constant speed propeller. The EV-55 is a STOL aircraft able to operate from paved and unpaved runway types and is designed and certified according to CS/FAR 23 regulation in a normal category. Fuselage is of a semi-monocoque metal structure with a share of composites and is characterized by large inner space. The wing of the EV-55 aircraft is integral, trapezoidal-shaped, all-metal structure with the composite aerodynamic wing tips. In the wing between spars there are integral fuel tanks. The wing is equipped with split Fowler wing flaps and ailerons. Currently, project is staged at the point of 1st stage of the prototype flight testing.

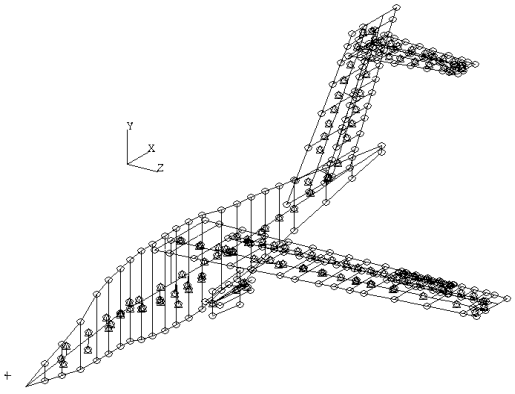

Fig.8. Structural FE model

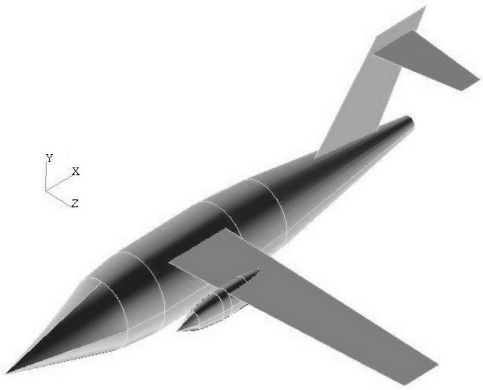

Fig.9. Aerodynamic FE model

FE model is prepared as a dynamic beam model. Stiffness characteristics are modeled by means of the massless beam elements, inertia characteristics are modeled by concentrated mass elements. Flexible engine attachment and the control surfaces drives are realized by spring elements. Model includes also various conditions and auxiliary elements (controls suspension, visualization etc.). Model is prepared as a half-model with half values at the plane of symmetry and the symmetric or antisymmetric boundary condition. There are various options considering the fuel loading, fuselage loading, controls balancing, etc. prepared. Aerodynamic model is based on the Wing Body Interference Theory. Wing, vertical and horizontal tail are modeled by means of Doublet – Lattice panels, fuselage and nacelle as Slender and Interference bodies. Controls and tabs are modeled separately. Aerodynamic model includes also correction for the propeller slipstream. Interpolation of both structural and aerodynamic model is realized by means of the beam splines. The structural and aerodynamic

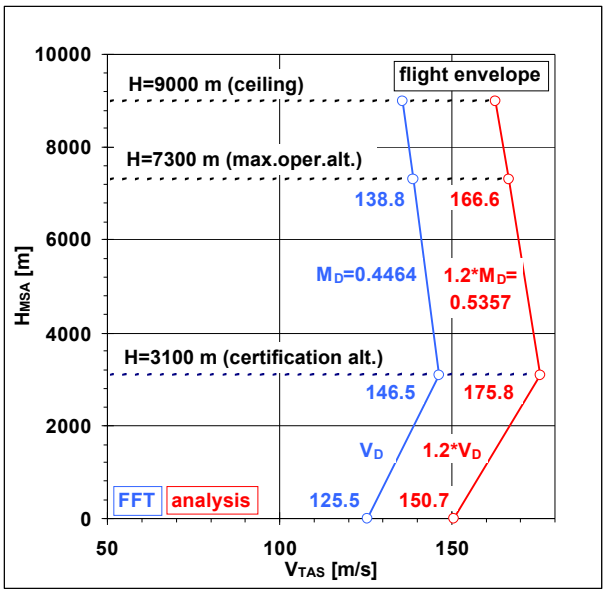

Fig.10. Flight envelope (V-H)

model is presented in the fig.8 and fig.9 respectively.

Each set of analyses was started by the standard analysis for a nominal state, and then a set of the optimization analyses followed. For the nominal states, no whirl flutter instability was found. The frequency ratio values were selected in order to well describe the stability boundaries. Both frequency orders, it means $f_H > f_V$, and $f_V > f_H$ were taken into account. The range of the frequency ratios was set according the experiences from the previous Czech aircraft

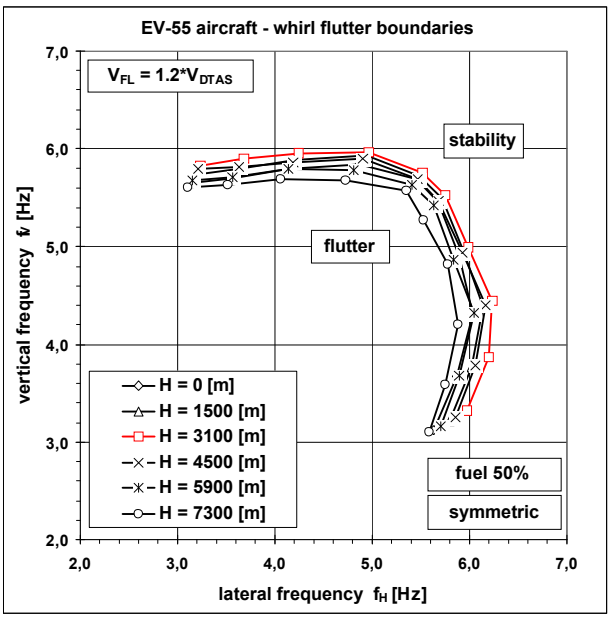

Fig.11. Stability boundaries – fuel loading: 50%; symmetric; parameter – flight altitude H

structures with a similar engine attachment system (Ae-270 and L-410).

There were 15 modes for the symmetric boundary condition and 20 modes for the antisymmetric boundary condition included into the stability analysis. It covered the frequency range up to about 50 Hz.

In the first phase, analyses for fuel loading of 50% and the symmetric boundary condition with variation of the flight altitude (0; 1500; 3100; 4500; 5900; 7300) [m] were performed. The certification velocities were set according the flight envelope as ($1.2*V_D$) or ($1.2*M_D$) – see fig.10. The result stability boundary curves are presented in the fig.11. From these calculations, regarding the changes of

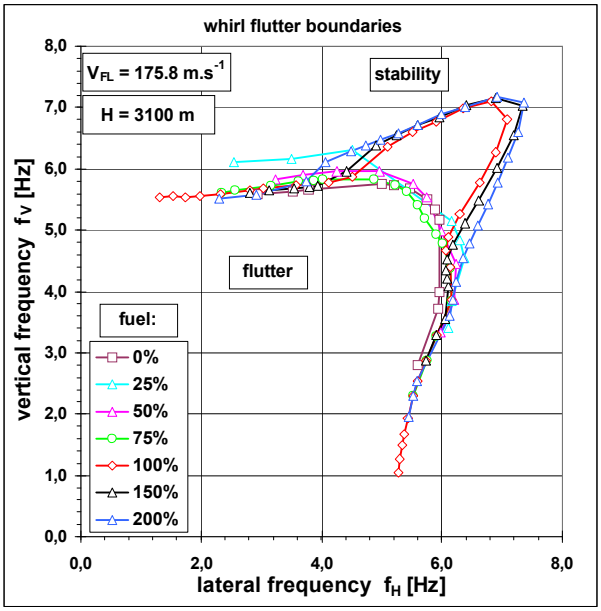

Fig.12. Stability boundaries – flight altitude H = 3100 [m]; symmetric; parameter - fuel loading

certification velocity, the critical altitude of H = 3100 [m] in terms of the whirl flutter was set. Further calculations were performed just for the altitude of H = 3100 [m].

The parameter of the next analyses was the fuel loading (0; 25; 50; 75; 100) %. Calculations were performed for both symmetric and antisymmetric boundary conditions. The result stability boundaries for the symmetric boundary condition are presented in the fig.12. Regarding the change of the boundary character for the fuel loading of 100 % in comparison with the other ones, the calculations of artificial fuel loading of

150% and 200% for a symmetric boundary condition were added. The character of the stability boundary is determined by the frequency distance between the engine vibration mode and residual structure mode, e.g. 1st wing bending mode of the optimized structure. The flutter frequencies vs. frequency ratios are presented in the fig.13.

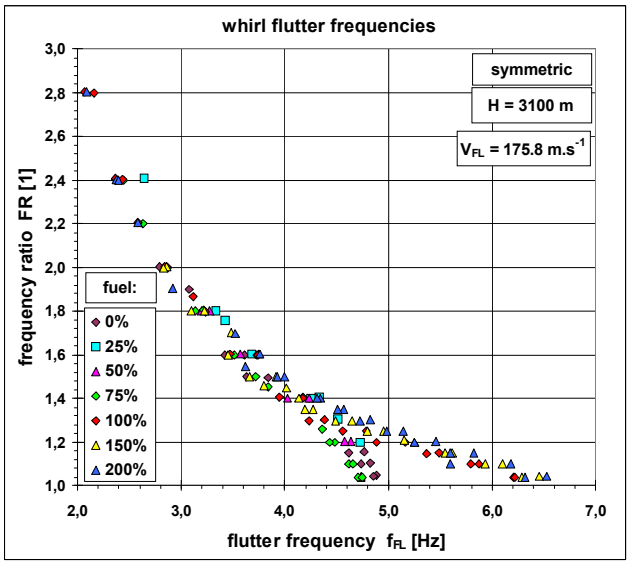

Fig.13. Flutter frequencies – flight altitude H = 3100 [m]; symmetric; parameter - fuel loading

There is documented the influence of the fuel loading to the selected natural frequencies in the fig.14. There are visible the nominal engine vibration frequency ratios vs. fuel loading level. The frequency ratios are varying between values of 1.26 and 1.02. It is noticeable, that the engine horizontal frequency is affected much more then the vertical one. For the artificial fuel loading of 150% and 200%, the frequency order was changed.

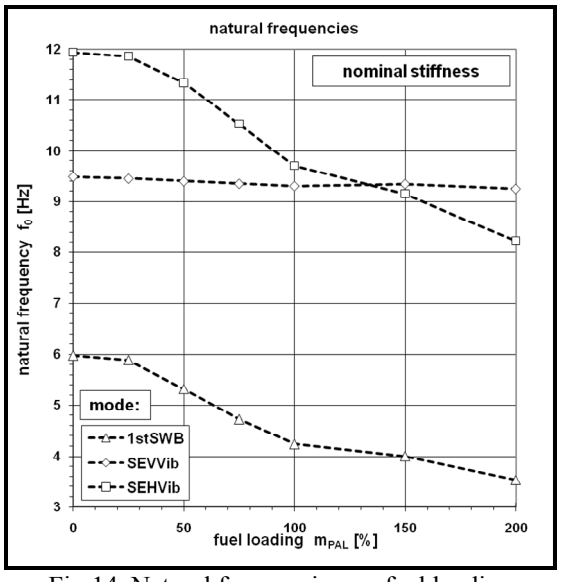

Fig.14. Natural frequencies vs. fuel loading

All above mentioned analyses were performed considering no downwash effect. The downwash and sidewash effect was evaluated for selected fuel loading levels of (50; 100; 200) % and the symmetric boundary condition. Calculations were performed for the same frequency ratios as the no downwash ones in order to make a comparison of both results. Influence of the downwash was evaluated by means of the relative value of the square root of the sum of the both frequency differences squares:

$$\Delta dnws = \frac{\sqrt{\left(f_{Vdnws} - f_V\right)^2 + \left(f_{Hdnws} - f_H\right)^2}}{\sqrt{f_V^2 + f_H^2}}.100 \quad (11)$$

The results shows, that the influence of the downwash may be quite significant. The maximum value of Δdnws was found on the level of 8.69%. The effect of the downwash is destabilizing. The influence of the downwash is strongly dependent on the dynamics of the whole structure. It was found, that the higher distance between the wing bending frequency and the engine vibration frequencies makes a higher level of the downwash influence (see

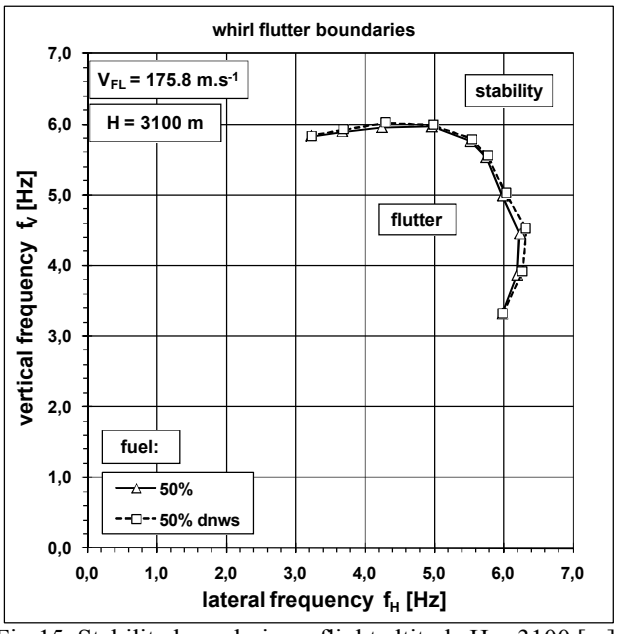

Fig.15. Stability boundaries – flight altitude H = 3100 [m]; symmetric; fuel loading 50%; influence of downwash

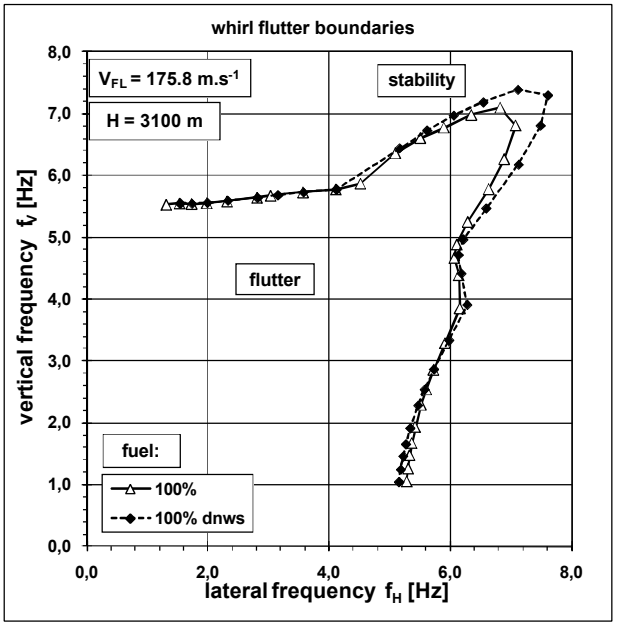

Fig.16. Stability boundaries – flight altitude H = 3100 [m]; symmetric; fuel loading 100%; influence of downwash

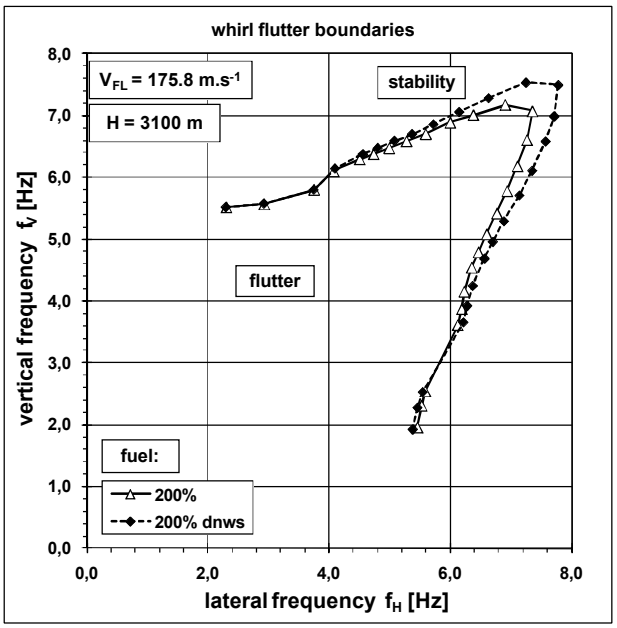

Fig.17. Stability boundaries – flight altitude H = 3100 [m]; symmetric; fuel loading 200%; influence of downwash

fig.16 and 17). On the other side, provided the distance between the wing bending and engine vibration frequencies is small, the influence of the downwash is negligible (see fig.15).

7 Conclusion

Submitted paper presents a practical application of the procedure for determination of the critical values of parameters regarding the whirl flutter stability on the real aircraft structure. An optimization-based solution is employed. Parameters are stiffness of the engine suspension or engine vibration modes natural frequencies respectively. Determination of these values, it means the values when the whirl flutter speed is equal to the certification speed would allow replacing large parametric studies varying the stiffness. It would considerably decrease number of necessary analyses, particularly for the twin wing-mounted engine aircraft, when the number of secondary parameters, like wing inertia and stiffness must be included as well. Obviously, it would allow moving the whirl flutter analysis to the early phase of the aircraft development, since it requires no experimental data. After the ground vibration tests, just rate of reserve towards the critical values would be evaluated. Such approach would significantly improve the effectiveness of the certification process.

The procedure was exploited during the certification analyses of the new Czech EV-55 twin turboprop utility aircraft. For the nominal parameters, there was found no whirl flutter instability. The stability boundaries for the certification speed have been drawn for various secondary parameters options. After the ground vibration test of the prototype planned to 2010, the measured engine vibration frequencies will be compared with the calculated critical ones and the rate of reserve will be evaluated.

8 Acknowledgement

The paper relates to the following research projects:

MSM 0001066903 “Research on Strength of Low-weight Structures with Special regard to Airplane Structures”;

6th FP EC Integrated Project „CESAR“ (Cost Effective Small Aircraft), Contract No.30888, Task 2.5 „Flutter Prevention for the Small Aircraft“.

References

[1] Ribner, H.S.: *Propellers in Yaw*, NACA Report 820, 1945

[2] Ribner, H.S.: *Formulas for Propellers in Yaw and charts of the Side – Force Derivatives*, NACA Report 819, 1945

[3] Houbolt, J.C. – Reed, W.H.: Propeller – Nacelle Whirl Flutter, *Journal Aerospace Sciences*, Vol.29, pp.333 – 346, 1962

[4] Forsching, H.W.: *Grundlagen der Aeroelastik (translation: Osnovy Aerouprugosti)*, Mašinostroenie Moscow, IB 3112, 1984

[5] Rodden, W.P. – Rose, T.L.: Propeller / Nacelle Whirl Flutter Addition to MSC/NASTRAN, *Proceedings of the 1989 MSC World User's Conference*, Universal City, Ca.,U.S.A., Paper No.12, March 1989

[7] Čečrdle, J.: Whirl Flutter Analysis of the Commuter Aircraft Aeroelastic Model Wing – Engine Component, *Proceedings of the Engineering Mechanics 2006, National Conference with International Participation*, 15.-18.5.2006, Svratka, Czech Republic, paper no.119, book of extended abstracts pp. 42 – 43, full text on CD-ROM, ISBN 80-86246-27-2

[8] Čečrdle, J.: Whirl Flutter Analysis of the Small Transport Aircraft, *Proceedings of the IFASD 07 (International Forum on Aeroelasticity and Structural Dynamics), International Conference*, Stockholm, Sweden, IF-021, CD-ROM

[9] Čečrdle, J.: Exploitation of Optimization Solution for Determination of Whirl Flutter Stability Boundaries, *Proceedings of the 26th Congress of the International Council of the Aeronautical Sciences (ICAS 2008), International Conference* September, 14 – 19, 2008, Anchorage, AK, USA, ICAS2008-P3.2

Copyright Statement